Sensors **2006**, *6*, 578-592

sensors

ISSN 1424-8220

http://www.mdpi.org/sensors

Full Research Paper

Development of an In-Fiber Nanocavity Towards Detection of Volatile Organic Gases

Cesar Elosua, Ignacio R. Matias*, Candido Bariain and Francisco J. Arregui

Departamento de Ingeniería Eléctrica y Electrónica, Universidad Pública de Navarra, Campus de Arrosadia s/n, 31006 Pamplona, Spain

E-mails: cesar.elosua@unavarra.es, natxo@unavarra.es, cba@unavarra.es, parregui@unavarra.es

* Authors to whom correspondence should be addressed; e-mail: natxo@unavarra.es; Phone: +34 948169288, Fax.: +34 948169720

Received: 29 March 2006 / Accepted: 14 June 2006 / Published: 16 June 2006

Abstract: A fiber optic sensor for Volatile Organic Compounds (VOCs) detection has been developed and characterized for some organic gasses. The sensor is based on a novel vapochromic material, which is able to change its optical properties in presence of organic vapors in a reversely way. A nano Fabry Perot is constructed onto a cleaved ended optical fiber pigtail by Electrostatic Self Assembly method (ESA), doping this structure with the vapochromic material. Employing a reflection scheme, a change in the intensity modulated reflected signal at 850 nm have been registered. The response of the sensor has been evaluated for five different VOCs, and a deeper study has been made for vapors of three different alcohols.

Keywords: Fiber optic sensor, Volatile Organic Compound, Vapochromic complex, Electrostatic Self Assembly method, nanocavity

---

1. Introduction

It is well known that organic volatile compounds detection is an important aim in sensor technology. There are many and assorted fields where these kind of sensors are demanded, just to mention a few, environmental applications [1], electronic noses [2, 3], chemical industry [4] or non invasive food analysis [5]. For the development of these applications, electronic sensors have been mostly used. Most of these sensors are based on the VOC absorption of a polymer [6], which depends

on some factors, such as the organic vapor concentration, the chemical properties of polymer and its reactivity with the solvent among others. Some examples of these devices are Surfaces Acoustic Wave (SAW) [7] or capacitive sensors [8], just to mention a couple.

Fiber optic sensors came on this scene just fifteen years ago [9], offering some important advantages versus electronic ones that have motivated their investigation and development. Their electromagnetic immunity is one of the most important, because they can be used in high noisy ambient where the electronic ones have serious operating problems. Besides, they are passive devices, so no electric power is need in the sensing zone, which is very important in atmospheres with a high inflammable complex concentration. Other interesting properties are their small size and light weight, remote operation or capability of multiplexing [10].

Taking advantage of great potential that fiber optic sensors offer, a novel vapochromic material, whose optical properties change reversely in presence of organic vapors, has been employed to develop an optical fiber volatile organic compounds sensor. A nanocavity doped with this material is deposited following the ESA protocol [11], which can be implemented in an automated way, offering a great reproducibility. Furthermore, this process has been made chemically compatible with the vapochromic material, so it keeps its original optical characteristics during and after the deposition process.

2. Experimental Set-up

A multimode optical fiber with core and cladding diameters of 62.5 and 125 μm respectively was chosen to fabricate the sensor. A pigtail of this fiber is cut at one end with a Siemens S46999-M9-A8 precision fiber cleaver. A nanocavity doped with the vapochromic material is deposited onto this cleaved end; in other studies, this small size has shown very important advantages [12].

The same reflection experimental set up, which is shown in figure 1, has been used for both sensor construction and response analysis. The sensor head is connected to the port 2 of a directional Y 50:50 coupler, while a light source is connected to port 1and a photodetector is connected to port 3. So, the optical power from the source goes through port 1 and reaches the sensor head; the reflected optical power gets the coupler back reaching the detector. Just to reduce insertion loss, all optical devices have a 62.5 μm core diameter.

During the nanocavity construction process, the fiber end is stayed on air. When studying the response of the sensor in presence of different VOCs, the sensor head is introduced into a chamber closed hermetically, which dimensions are 9 cm of diameter, 2 cm high, and a volume of 275 cm^3, inside where the organic solvents are injected in liquid phase.

3. Nanosensor construction

3.1. Vapochromic material

The working principle of most chemical fiber optic sensors is based on the modulation of the fiber guided light intensity produced by a change in the optical properties of a sensing substance [13]. Because of that, for the preparation of detectors of VOCs, complexes able to achieve such changes

reversely are required. A new chemistry branch, the organometallic one, offers complex compounds with some interesting and particular properties.

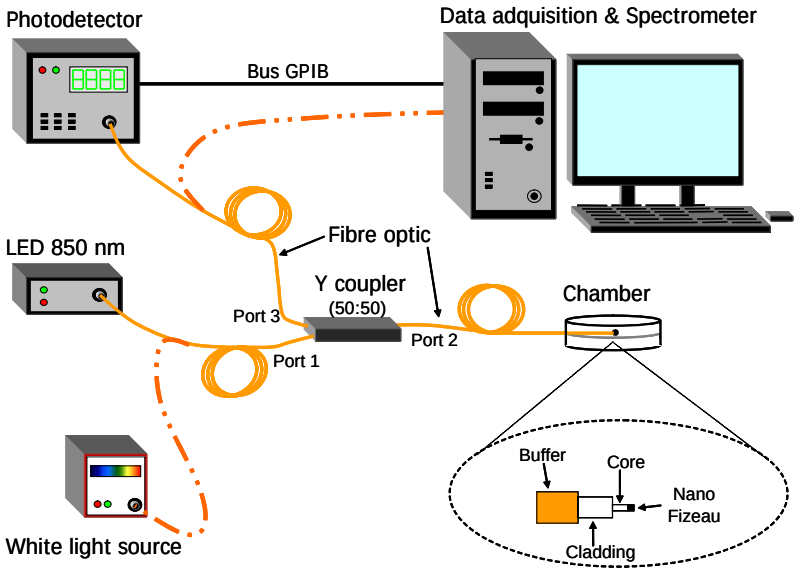

Figure 1. Experimental set-up arranged in order to register the nanocavity construction and the variation in the reflected optical power when exposed to VOCs (fiber optic solid line), and to record the absorbance spectra (fiber optic dotted line).

Organometallic compounds are polymer chains which monomers are linked by metal transition atoms, instead of non metallic ones [14]. Metals such as gold, silver or palladium has been used to synthesize these types of complexes, and have interesting potential applications. In this case, the organometallic complex suffers a change in their optical properties (refractive index and colour) in presence of VOCs, which is easy to detect with the set up shown in the previous section.

The term vapochromic was used first by Nagel and Mann and co-workers, and with it palladium-platinum complexes whose colour changed in presence of VOCs were described [15, 16]. The vapochromic material employed in this work belongs to a family of complexes of general formula $[Au_2Ag_2(C_6F_5)_4L_2]_n$, where L can be pyridine, 2,2'bipridine, 1,10 phenantroline, ½ diphenylacetylene and other ligands. In presence of coordinating solvents as acetone, alcohols or acetic acid, first, the polynuclear structure of the starting complex disappears, getting broken the gold-silver and gold-gold bounds, which are responsible for the initial colour; then, a new anion-cation derivate is formed as a consequence of the solvent coordination to the silver centres (see figure 2), provoking a change in the colour of the complex. Some preliminary fiber optic sensors based on this family of complexes have been already presented and characterized for VOCs detection [17, 18].

In this work, the vapochromic complex is based on pyridine ligands. This product is presented in form of bright red powders, and shows fluorescence at 580 nm when illuminated with a 380 nm light source. Although there is necessary an important quantity of organic solvent to induce a full colour change, in presence of small quantities of solvent in vapour phase, a detectable change in refractive index is produced.

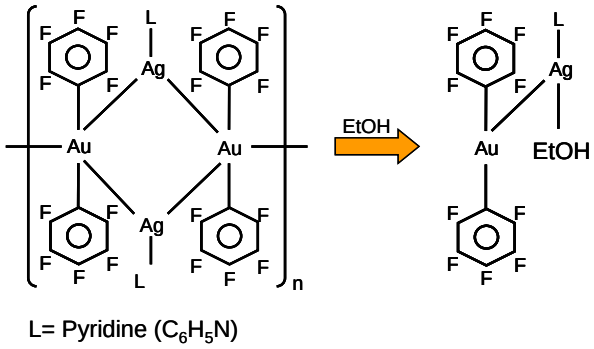

Figure 2. Molecular structure of the vapochromic material employed and its reaction in presence of ethanol vapours.

3.2. Electrostatic self-assembly method

An automated method to fix the vapochromic material onto the cleaved end pigtail is desirable to obtain reproducible sensors. Among deposition techniques such as sol-gel [19, 20], dip coating [21] or Langmuir-Blodgett [22], the ESA method offers simplicity and reproducibility [23]. Besides, many materials have been properly deposited with this technique [24]. When used on fiber optic, Fabry-Perot nanocavities with lengths bellow a micrometer can be build-up.

The ESA is an iterative method, so it can be easily automated with a programmable robot. Firstly, the substrate used (in this case fiber optic), has to be chemically cleaned dipping it into a mixture of sulphuric acid and hydrogen peroxide (3:1) for five minutes, which also induces a negative charge on the surface of the fiber. After this, a cyclic process begins: the substrate is submerged first into a cationic polymeric solution, so a cationic monolayer is deposited on the substrate by electrostatic attraction; then, the substrate is dipped into an anionic polymeric solution. The negative charged monolayer is diffused into the positive ones [25], yielding into an optically homogenous bilayer; this means that the refractive index can be consider homogeneous in the assembled bilayer; as the final deposition consists of n bilayers of homogeneous refractive index, it can be considered as a nanocavity in stead of a grating. In figure 3 it is shown the basic synthesis process. The polymers employed and the chemical variables for the charged solutions determine the resulting coating properties.

In our work, a solution of poly allylamine hidrocloride (PAH) was used as the polycation, and poly acrylic acid (PAA) as the polyanion. The ionization degree of these polymers solved in water can be modified varying the pH [26], producing also to a change in the properties of the nanocavity structure. Furthermore, the thickness of the final nano Fabry-Perot cavity obtained following the ESA method is shorter than the coherent length of LEDs, so this type of light source can be used instead of LASERs, with the advantages this implies.

These types of interferometric nanocavities have been already used as sensing mechanism in some optical fiber sensors, changing for example, their length or index of refraction as a function of humidity [27]. The interferometric response is produced by the two mirrors of the nanocavity (fiber-film and film-air interfaces). As the bilayers get deposited, the film grows, and hence, the reflected optical power changes following an interferometric (two beams) pattern. This interferometric behaviour gets much clearer when depositing more and more bilayers, as for example in references [30, 32].

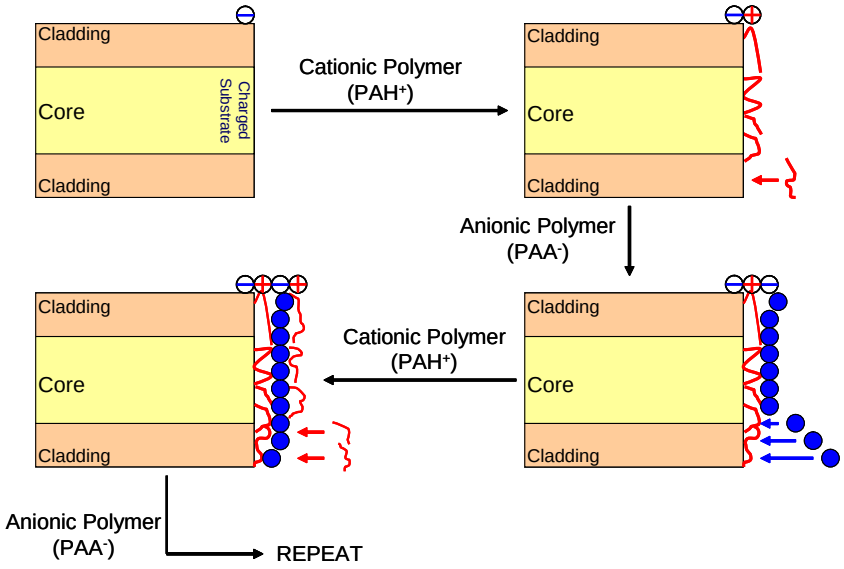

Figure 3. Schematic of the ESA deposition process onto the cleaved end of a fiber optic. The symbols are idealized and not intended to represent exactly the conformation of the polyelectrolyte chains.

3.3. Nanocavity construction

In previous studies we reported that the vapochromic material can be deposited applying the ESA method [29]. Although the sensing material is not soluble in water, a polymeric solution doped with vapochromic material can be obtained eventually, just dissolving it in ethanol. To prevent the vapochromic material degradation, it is added into the PAA solution, which is less reactive than the polycationic one. The pH of both polymeric solutions is 8; on one hand, an acid destruction of the vapochromic material is avoided, and on the other, if the solutions are set at the same acidity, construction problems in nanocavity are avoided.

The polycation and polyanion solutions are 10mM, and the proportion between the vapochromic complex and ethanol is 1mg/100 μl; 500 μl of this solution is added to 20 ml of water, mixing this last solution with the anionic polymer. With these relative amounts, the optical properties of the vapochromic material in solution are similar than in solid state.

The nano Fabry-Perot cavity consist of 25 bilayers build up at the end of a cleaved optical fiber pigtail. The structure is defined by the form $[PAH^{+}/PAA^{-}(Ethanol+Vap)]_n$, being n the number of bilayers (25 in this case). To cure the sensor, it was kept during 24 h at room temperature, in order to get the remaining ethanol in the sensor head surface evaporated.

With the set up shown in figure 1, the growing of the nanocavity can be followed, just registering the reflected optical power each time that a monolayer is deposited onto the end of the optical fiber. These measures will give a response similar to a Fabry-Perot interferometer [30], as can be seen in figure 4.The light source employed to monitor the growing of the nanocavity is a LED at 850 nm.

Some information about the size of the nanocavity can be inferred from figure 4; when the interference depends on the size of the cavity, the distant between two maximums or minimums of interference is half the wavelength the cavity is being excited with. In this case, half a period of

interferometric response is registered until bilayer number 25, which means that the length of the nanocavity is about 250 nm (a quarter of the wavelength used to excite it) [31].

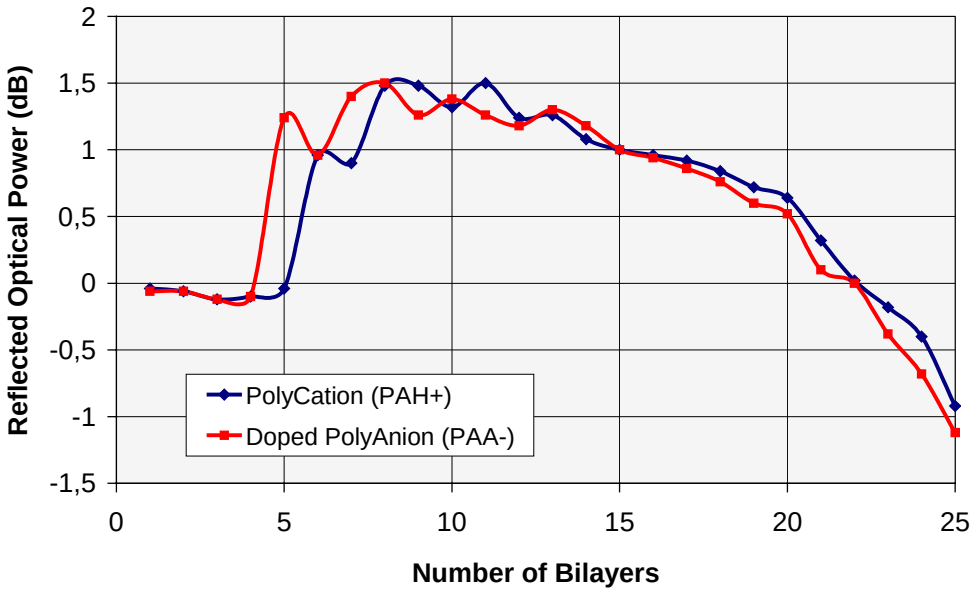

Figure 4. Construction curve of the nano Fabry-Perot for the polycation (PAH^+) and the polyanion (PAA^-) doped with the vapochromic material.

4. Characteristics of the sensor

Although the ambient factors sensitivity of the sensor has not been performed in this study, previous results obtained in our group with sensors developed using the ESA technique and the vapochromic material, showed that the response of the device has neither thermal or humidity correlation [17, 18]. Even in more complex sensing schemes and more suitable to be sensitive to temperature than in this case, it is showed that the cross sensitivity to temperature is negligible in the whole spectrum [32].

The characterization of the sensor has been made from two different points of views. First, analyzing its spectral response, and secondly obtaining the evolution of the reflected optical power from the sensor in presence of different VOCs, as in previous related works [18, 33].

4.1. Spectral analysis

Spectral study has been used with two different purposes. First, to measure the fluorescence of the vapochromic complex once it get fixed onto the cleaved ended fiber, by the emission spectra; and also to register the absorbance spectra of the sensor when exposed to different VOCs. This spectral analysis has been implemented using the reflection set up shown in figure 1. In this case, an USB2000-UV-VIS Miniature Fiber Optic Spectrometer purchased from Ocean Optics Inc. was connected to port 3, a LED at 380 nm was to connected to port 1 when measuring the fluorescence of the sensing complex, and in order to get the absorbance spectra, a white light source was connected to port 1 instead of a LED.

A. Vapochromic complex fluorescence

The fluorescence of the vapochromic material at 585 nm when illuminated with a 380 nm light has no sensitive purposes. It is used only to have an evidence that the optical properties of the vapochromic material have suffer no degradation during the deposition process, and that it has been successfully deposited onto the sensor head. In figure 5, the fluorescence of the vapochromic complex in different states is shown; there is a parasite fluorescence peak provoked by the optical fiber around 430 nm, but does not infer the one of the vapochromic complex.

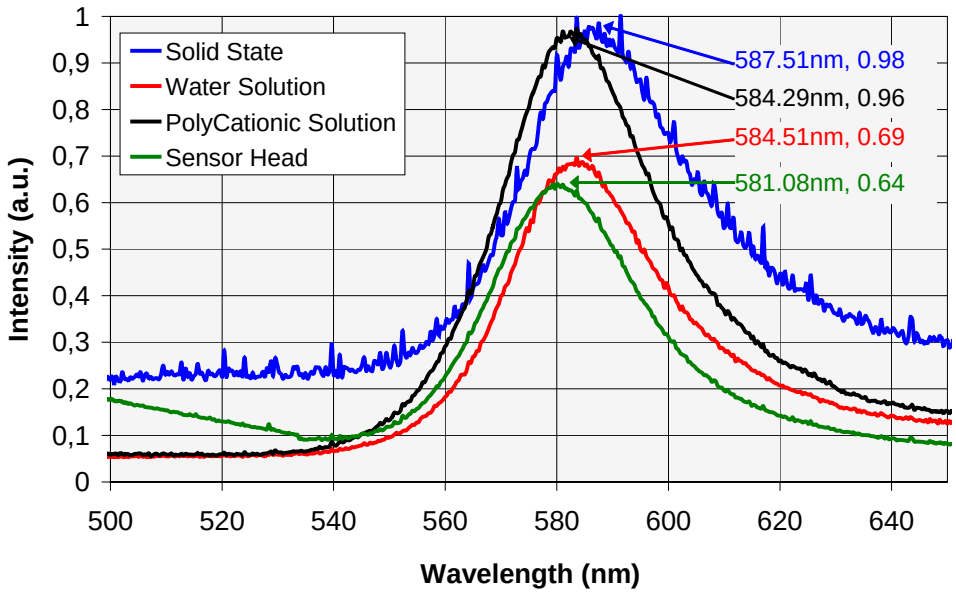

Figure 5. Fluorescence of the vapochromic material, exciting it with a 380nm LED, in different states.

B. Absorbance spectra

In this case, following the set-up shown in figure 1, the USB2000-UV-VIS spectrometer is connected to port 3, and a white light source is connected to port 1. In order to be consistent in all the experimental curves, the absorbance will be given in absorbance absolute units, which are defined as:

$$A = -\log\left(\frac{S_\lambda - D_\lambda}{R_\lambda - D_\lambda}\right) \quad (1)$$

where S_λ is the optical power received from the sample, D_λ the optical power of the dark reference signal, or dark noise, and R_λ the optical power monitored from the reference signal, all of them at wavelength of λ.

As a relative measure, the absorbance spectrum consists of the comparison between two absolutes values; in this case, the reflected optical power collected when the sensor is exposed to organic vapors at a certain wavelength ($S_\lambda - D_\lambda$), is compared with the reflected optical power registered at the same wavelength when the sensor is in a VOC – free atmosphere ($R_\lambda - D_\lambda$). In both cases, D_λ is the reflected optical power detected when no light is coupled to the system, eliminating so the background noise. It

is remarkable that the absorbance spectra obtained gives no information about the spectral response of the device, only about the change that the VOCs provoke on it.

The optical absorbance of the nanocavity when exposed to five different organic vapours is shown in figure 6. In order to obtain a saturated ambient inside the chamber, the concentrations in each case were 43 mmol/l per ethanol, 62.5 mmol/l per methanol, 20 mmol/l per isopropanol, 43.5 mmol/l per acetic acid and 27.81 mmol/l per dichloromethane. The ethanol curve is easily identifiable from the others because there is only a crossing point with the isopropanol curve, but several wide spectral interrogating regions available to be used to sensing purposes.

Sensors used in artificial odor recognitions systems must show different sensibilities for individual organic vapors [2, 3]. In this case, the sensibility to the three alcohols is higher than the one of acetic acid and dichloromethane, so this device could be combined with other sensors that show other sensibilities to develop a sensing matrix system.

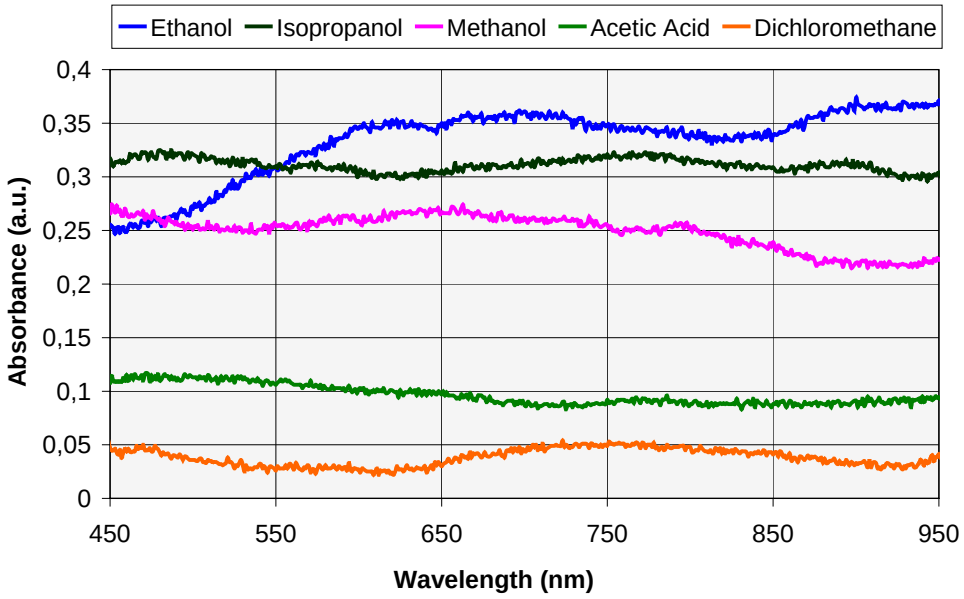

Figure 6. Absorbance spectra of the nanocavity when exposed to different VOCs. The measures were taken after 5 minutes of exposure.

As commented above, there is a wide spectral region where the optical interrogating signal could be used, giving the possibility of implementing a sensor network based on wavelength division multiplexion scheme in a straight forward way [10]. As can be seen from figure 6, a low cost LED emitting at 850 nm is a good choice to study the reflected optical power response when the sensor is exposed to organic vapors. Finally, it is remarkable that in all cases the spectra got stabilized in less than two minutes, providing a very repetitive sensor response and faster than others obtained with previous related implementations [29].

4.2. VOC assembly analysis

Once the sensor response was studied for a wide spectral region, the sensor was excited using a LED at 850nm, employing the configuration described in section 2. With this set up, changes in the

reflected optical power were recorded when the sensor head was exposed to different VOCs. After the optical fiber sensor head was placed inside the chamber, the organic compounds in liquid form were injected inside the chamber, and after a few minutes, the equilibrium liquid vapour was reached, so the atmosphere inside the chamber got saturated, and the vapours begun an adsorption process on the sensing nanocavity surface. This produces a change in the optical properties of the vapochromic material, and hence, in the reflected optical power. Once the reflected signal is stabilized, the chamber was opened and the optical power recovered its initial value almost immediately.

The concentrations employed for each VOC were the same that the ones used to study the absorbance spectra. The results obtained are shown in figure 7. For each vapour, two cycles were register in order to show the repetitive response of the sensor. If the doping vapochromic material concentration and the interrogating wavelength are fixed, it is possible to distinguish between different VOCs. Besides, the longer response time is almost two minutes in case of acetic acid, being shorter than 20 seconds when the sensitive nanocavity is exposed to isopropanol.

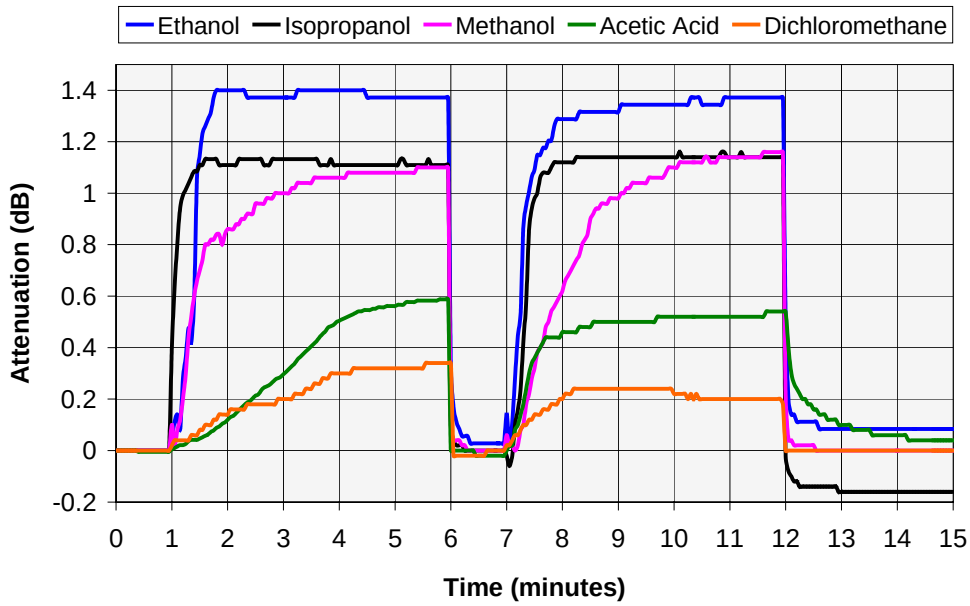

Figure 7. Attenuation of the reflected optical power when the sensor head is exposed to different VOCs and interrogated with a LED source at 850 nm.

The mechanisms governing the response and recovery times are quite different. Regarding rising times, it is affected by the vaporization process of the VOC and its sorption process by the sensitive material. On one hand, the organic compound is injected inside the chamber in liquid phase, so it needs time to get vaporized and to saturate the atmosphere; meanwhile, the vapor molecules initiate an adsorption process on the surface of the sensing head, provoking a change in the index of refraction of the vapochromic material, and hence, in the reflected optical power. So, using the experimental set-up of figure 1, time response depends on both, velocity of the vaporization of the VOC, and on the kinetic of the adsorption process on the sensor head. Nevertheless recovery time is much shorter because once the chamber is open, the VOC inside it leaves the chamber almost immediately.

As it can be seen in figure 7, and later on in figures 8 to 10, when the sensor head is exposed individually to VOCs, the change obtained in the reflected optical power is different for each case in

terms of attenuation (which depends on the changes in the refractive index provoked by each VOC) and time response (governed by both the vaporization process and the VOC diffusion kinetic onto the sensor head). So, chemical properties of the VOC determine the response for each organic vapor analyzed, and hence, an individual VOC may be estimated by measuring attenuation and time response, but never in case of gas mixtures.

From the experimental results presented in figure 7, it is possible to infer that the sensor developed is sensitive to at least 5 different VOCs, so the sensor head itself can not be used to handle organic vapor mixtures; but this low selectivity is desirable to perform an artificial odor recognition system, as has been already demonstrated in several electronic noses.

The sensitive material employed in this work belongs to a family of vapochromic complexes (whose members only differs on chemical ligands) that have been probed to have sensing properties similar to the one shown here (fast response to different VOCs and low selectivity). So although it can not be used to handle VOCs mixtures, it may be used to perform a sensor array system. Data treatment such neural networks or PCA algorithms for systems based in sensors arrays are well know and have been used successfully to identify different gas mixtures (odors) from different nature. In this field, the sensor developed offers a great potential use.

4.3 VOC individual analyse

Finally, the sensor response was studied for different concentrations of ethanol, methanol and isopropanol vapours in order to complete its characterization. To achieve this, the same process presented previously was used, but using three different concentrations for each organic solvent.

The response for ethanol concentrations of 54 mmol/l, 43 mmol/l and 21.5 mmol/l are shown in figure 8, showing in figure 8a the response time when the chamber is closed. In figure 8b, it can be distinguish the recovery time. The maximum difference in terms of stabilized optical power after each concentration cycle is of only 0.2 dB, and can be treated with methods already mention in the previous paragraphs. When working with different concentrations of a single VOC, the time response can be then used to distinguish between the different samples because the more concentration, the faster is the time response.

The same tests were implemented for different methanol and isopropanol concentrations, and the results are shown in figure 9 and figure 10 respectively.

5. Conclusions

An optical fiber nanosensor has been developed doping an interferometry Fabry-Perot based nanocavity constructed following the ESA method with a novel vapochromic material. The deposition method was automated, so a high reproducibility is guaranteed. Using a cleaved end multimode fiber, the complete implementation process takes only one day. The sensor head thus fabricated is able to distinguish among some VOCs and also can determinate different concentrations individually. Changes up to 1.44 dB in the reflected optical power were registered in less than two minutes. The response registered from the sensor in terms of time response and dynamic range for different VOCs and different concentrations, meet the conditions required to conform a sensor array system, and hence, it can be potentially used in order to performance an artificial odor recognition system.

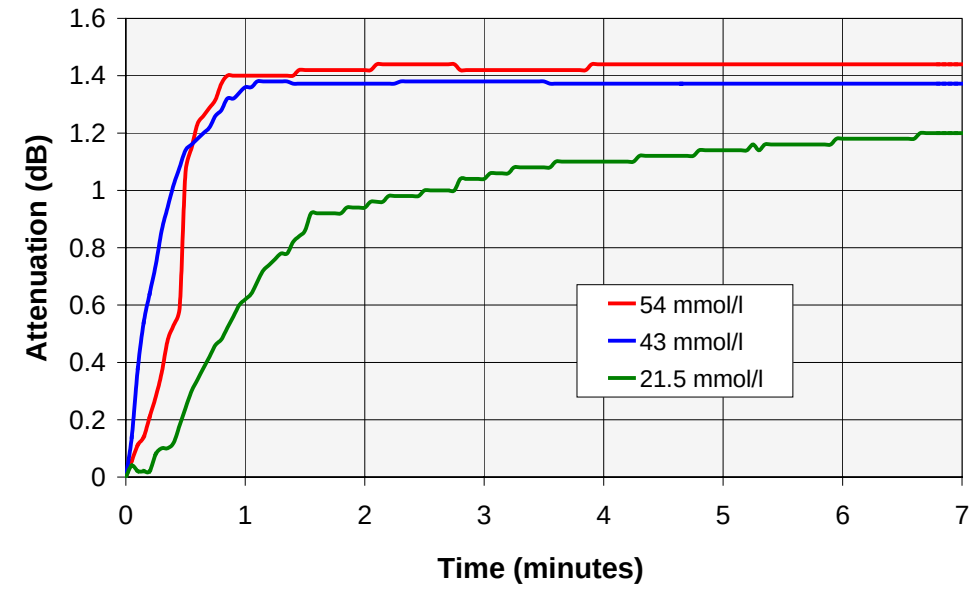

(A)

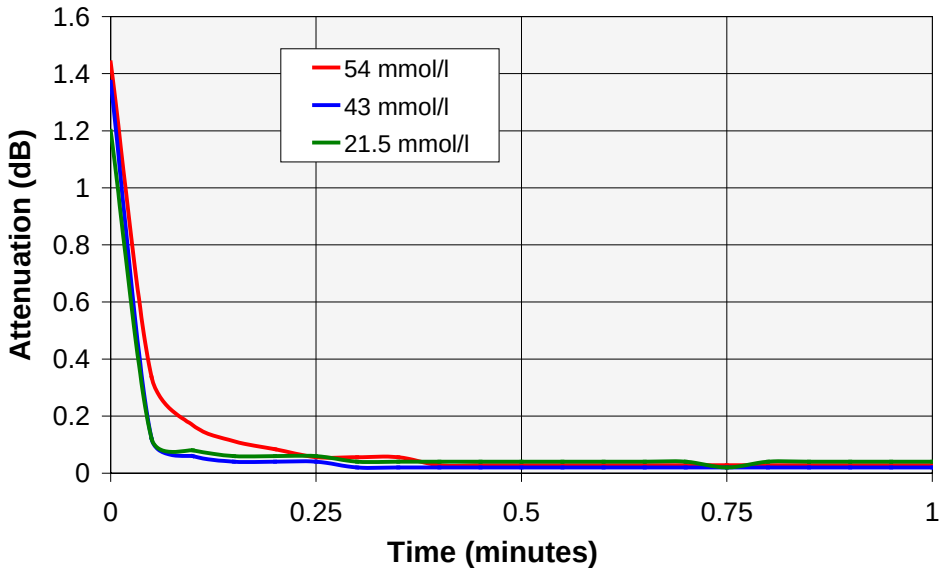

(B)

Figure 8. **(a)** Detail of the rise and stabilization of the optical reflected power when the response of the sensor when exposed to different ethanol concentrations. **(b)** Detail of the fall response of the sensor when the chamber is opened showing the recovery of the initial power level.

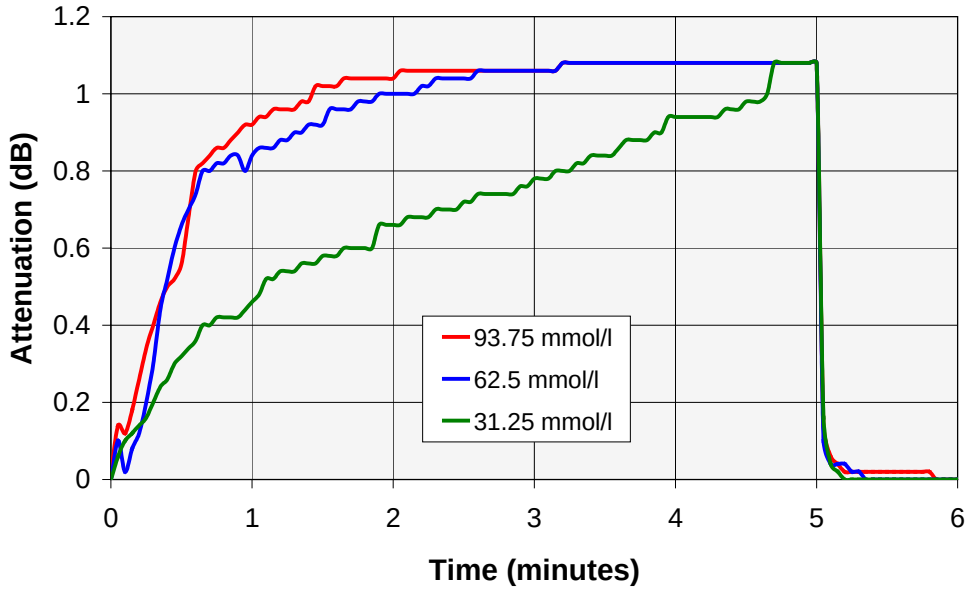

Figure 9. Response of the sensor when exposed to three different concentrations of methanol.

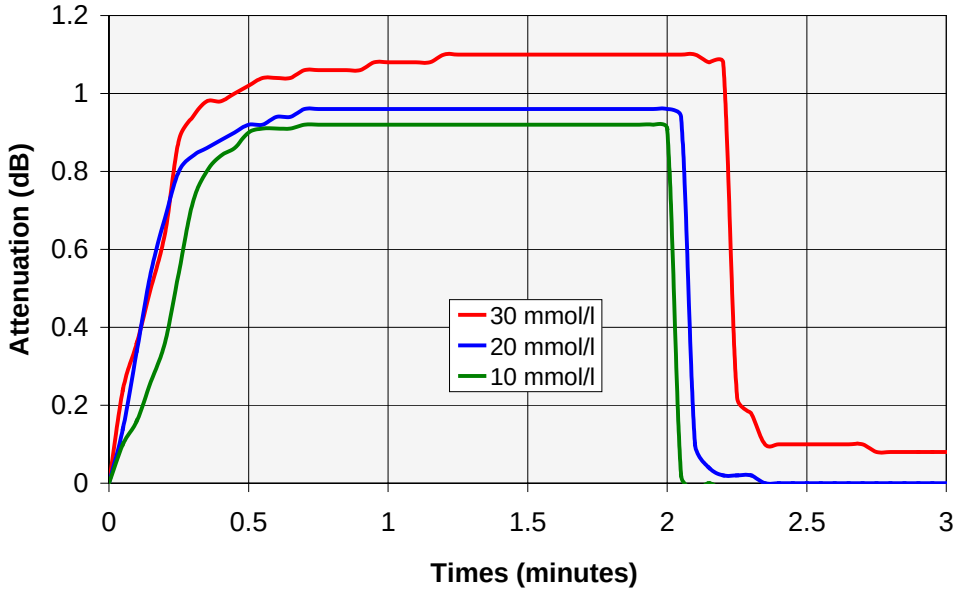

Figure 10. Response of the sensor when exposed to three different concentrations of isopropanol.

Acknowledgements

This work was supported by Spanish Ministerio de Ciencia y Tecnología and FEDER Research Grants CICYT-TIC 2003-000909 and CICYT-TEC 2004-05936-C02-01/MIC.

References and Notes

1. Delpha, C.; Lumbreras, M.; Siadat, M. Discrimination and identification of a refrigerant gas in a humidity controlled atmosphere containing or not carbon dioxide: application to the electronic nose. *Sensors and Actuators B* **2004**, *98*, 46–53.
2. D'Amico, A.; Di Natale, C.; Macagnano, A.; Davide, F.; Mantini, A.; Tarizzo, E.; Paolesse, R.; Boschi, T. Technologies and tools for mimicking olfaction: status of the Rome "Tor Vergata" electronic nose. *Biosensors & Bioelectronics* **1998**, *13*, 711–721.
3. S. Ampuero, J.O. Bosset, The electronic nose applied to dairy products: a review. *Sensors and Actuators B* **2003**, *94*, 1–12.
4. Gouws, G.J.; Gouws, D.J. Analyte identification using concentration modulation and wavelet analysis of QCM sensors. *Sensors and Actuators B* **2003**, *91*, 326–332.
5. Brezmes, J.; Llobet, E.; Vilanova, X; Saiz, G.; Correig, X. Fruit ripeness monitoring using an Electronic Nose. *Sensors and Actuators B* **2000**, *69*, 223–229.
6. Lonergan, M.C.; Severin, E.J.; Doleman, B.J.; Beaber, S.A.; Grubbs, R.H.; Lewis, N.S. Array-based vapor sensing using chemically sensitive carbon black-polymer resistors. *Chemical Materials* **1996**, *8*, 2298–2312.
7. Yang, Y.; Yang, P.; Wang, X. Electronic nose based on SAWS array and its odor identification capability. *Sensors and Actuators B* **2000**, *66*, 167–170.
8. Delapierre, G.; Grange, H.; Chambaz, B.; Destannes, L. Polymer-based capacitive humidity sensor: characteristics and experimental results. *Sensors and Actuators B* **1983**, *4*, 97–104.
9. El-Sherif, M. A. On-Fiber sensor and modulator. *IEEE Transactions on Instrumentation and Measurement* **1989**, *38*, 595–598.
10. Achaerandio, E.; Jarabe, S.; Abad, S.; Lopez-Amo, M. New WDM Amplified Network for Optical Sensor Multiplexing. *IEEE Photonics Technology Letters* **1999**, *11*, 1644-1946.
11. Decher, G. Fuzzy Nano Assemblies: toward layered polymeric multicomposites. *Science* **1997**, *277*, 1232-1237.
12. Kolle, C.; Gruber, W.; Trettnak, W.; Biebernik, K.; Dolezal, C.; Reininger, F. Fast optochemical sensor for continuous monitoring of oxygen in breath–gas analysis. *Sensors and Actuators B* **1997**, *38*, 141–149.
13. Grattan, K.T.V.; Sun, T. Fibre optic sensor technology: an overview. *Sensors and Actuators A* **2000**, *82*, 40–61.
14. Usón, R.; Laguna, A.; Laguna, M.; Manzano, B. R. Syntesis and Reactivity of Bimetallic Polyfluorophenyl Complexes; Crystal and Molecular Structures of [{AuAg(C6F5)2(SC4H8)}n] and [{AuAg(C5F5)2(C6H6)}n]. *Chemical Society Dalton Trans* **1984**, 285-292
15. (a) Nagel, C.C. *U.S. Patent* **4,826,774**; (b) Nagel, C.C. *U.S. Patent* **48,349,093**.
16. Buss, C.E.; Anderson, C.E.; Pomije, M.K.; Luzt, C.M.; Britton, D.; Mann, K.R. Structural investigations of vapochromic behaviour – X-ray single-crystal and powder diffraction studies of [Pt(CN-iso-C3H7)4][M(CN)4] for M= Pt or Pd. *Journal of the American Chemical Society* **1998**, *120*, 7783-7790.

17. Bariain, C.; Matias, I. R.; Fernandez-Valdivielso, C.; Elosua, C.; Luquin, A.; Garrido, J.; Laguna M. Optical fibre sensors based on vapochromic gold complexes for environmental applications. *Sensors and Actuators B* **2005**, *108*, 535-54.
18. Luquin, A.; Bariain, C.; Vergara, E.; Cerrada, E.; Garrido, J.; Matias I. R.; Laguna, M. New preparation of gold–silver complexes and optical fibre environmental sensors based on vapochromic[Au2Ag2(C6F5)4(phen)2]n. *Applied Organometallic Chemistry* **2005**, *19*, 1232–1238.
19. Grant, S. A.; Satcher J. H. Jr.; Bettencourt, K. Development of sol–gel-based fiber optic nitrogen dioxide gas sensors. *Sensors and Actuators B* **2000**, *69*, 132–137.
20. Lobnik, A.; Majcen, N.; Niederreiter, K.; Uray, G. Optical pH sensor based on the absorption of antenna generated europium luminescence by bromothymolblue in a sol - gel membrane. *Sensors and Actuators B* **2001**, *74*, 200-206.
21. Arregui, F.J.; Otano, M.; Fernández-Valdivielso, C.; Matias, I.R. An experimental study about the utilization of Liquicoat® solutions for the fabrication of pH optical fibre sensors, *Sensors and Actuators B* **2002**, *87 (2)*, 291-297.
22. Bariain, C.; Matias, I.R.; Fernandez-Valdivielso, C.; Arregui, F.J.; Rodriguez-Mendez, M.L.; de Saja, J.A. Optical fiber sensor based on lutetium bisphthalocyanine for the detection of gases using standard telecommunication wavelengths, *Sensors and Actuators B* **2003**, *93*, 153–158.
23. Arregui, F.J.; Latasa, I.; Matias, I.R.; Claus, R.O. An optical fiber pH sensor based on the electrostatic self-assembly method, *Proceedings of the Second IEEE Sensors Conference* **2003**.
24. Lenahan, K.M.; Wang, Y.-X.; Liu, Y.; Claus, R.O.; Heflin, J.R.; Marciu, D.; Figura, C. Novel polymer dyes for nonlinear optical applications using ionic self assembled monolayer technology, *Advanced Materials* **1998**, 853–855.
25. Zhanga, J.; Sengera, B.; Vautiera, D.; Picarta, C.; Schaafc, P.; Voegela, J.C.; Lavallea, P. Natural polyelectrolyte films based on layer-by layer deposition of collagen and hyaluronic acid. *Biomaterials* **2005**, *26*, 3353–3361.
26. Choi, J.; Rubner, M.F. Influence of the degree of ionization on weak polyelectrolyte multilayer assembly, *Macromolecules* **2005**, *38*, 124–166.
27. Arregui F. J.; Cooper K. L.; Liu Y. J. Optical fiber humidity sensor with a fast response time using the ionic self-assembly method, *IEICE Transactions on electronics*, **2000**, *E83C (3)*, 360-365.
28. Arregui, F. J.; Matías, I. R.; Claus, R. O. Optical fiber gas sensors based on hydrophobic alumina thin films formed by the Electrostatic Self-Assembly Monolayer process, *IEEE Sensors Journal*, **2003**, *3*, 56-61.
29. Elosua, C.; Bariain, C.; Matias, I. R.; Arregui, F. J.; Luquin, A.; Laguna, M. Volatile alcoholic compunds fibre optic nano sensor, *Sensors and Actuators B* **2005**, *115*, 444-449.
30. Yoshino, T.; Kurosawa, K.; Itoh, K.; Ose, T. Fiber-Optic Fabry-Perot Interferometer and Its Sensor Applications, *IEEE Journal of quantum electronics* **1982**, *18 (10)*, 1624-1633.
31. Arregui, F. J.; Matias, I. R.; Liu, Y.; Lenahan, K. M.; Claus, R. O.; Optical fiber nanometer-scale Fabry–Perot interferometer formed by the ionic self-assembly monolayer process, *Optics Letters*, **1999**, *24 (9)*, 596-598.

32. Arregui, F. J.; Richard, O. C.; Cooper, K. L.; Fernández-Valdivielso, C.; Matias I. R. Optical Fiber Gas Sensor Based on Self-Assembled Micrograting. *IEEE Journal of Lightwave Technology*, **2001**, *19*, 1932-1937.
33. Casado, S.; Elosúa, C.; Bariain, C.; Segura, A.; Matias, I.R.; Fernandez, A.; Luquin, A.; Garrido, J.; Laguna, M. A volatile-organic-compound optic-fibre sensor using a gold-silver vapochromic complex, *Optical Engineering* **2006**, *45 (4)*, 044401.